Fitoterapia 130 (2018) 94–99

Contents lists available at ScienceDirect

Fitoterapia

journal homepage: www.elsevier.com/locate/fitote

Antinociceptive effect of neo-clerodane diterpenes obtained from *Baccharis flabellata*

Matías Funes[a], María F. Garro[b,c], Rodrigo D. Tosso[b], Alejandra O. Maria[b], José R. Saad[b], Ricardo D. Enriz[b,c,*]

[a] INTEQUI-CONICET, Universidad Nacional de San Luis, Área de Química Orgánica, Almirante Brown 1455, D5700HGC San Luis, Argentina
[b] Facultad de Química, Bioquímica y Farmacia, Universidad Nacional de San Luis, Chacabuco 915, 5700 San Luis, Argentina
[c] Instituto Multidisciplinario de Investigaciones Biológicas (IMIBIO-CONICET), Chacabuco 915, 5700 San Luis, Argentina

ARTICLE INFO

Keywords:
Baccharis flabellata
Furan neoclerodane
Diene-acid clerodane dimer
Agonists of *kappa* receptors

ABSTRACT

We report here for the first time antinociceptive effects of extracts from *Baccharis flabellata*. Two extracts in this analysis, one obtained in summer and the other during winter time. Our results indicate that both extract show strong antinociceptive effects, being the extracts obtained during the summer significantly more active.

Our results suggest that this activity is mainly due to the presence of the diene-acid clerodane ent-15,16-epoxy-19-hydroxy-1,3,13(16),14-clerodatetraen-18-oic acid (DAC) and its dimer called DACD. Employing naloxone as an antagonist of opioid receptors, we demonstrated that both compounds act on opioid receptors, being the antinociceptive effect of DACD stronger than DAC. Thus, the antinociceptive activity of DACD was almost two times stronger than DAC (44.8 over 24.6 s in the hot-plate test) after one hour of treatments.

In order to better understand the mechanism of action at molecular level of these compounds, we conducted a molecular modeling study analyzing the molecular interactions of DAC and DACD complexes with the κ-ORs. Our results suggest interactions for both DAC and DACD with Gln115, Val118, Tyr119, Asn122 and Tyr313 stabilizing their complexes; however, these interactions are significantly stronger for DACD with respect to DAC. This finding could explain why DACD have a higher affinity for the κ-ORs. These results are in agreement with the obtained antinociceptive effect. In addition, our results indicate that these neoclerodanes would have a mechanism of action similar to that of salvinorin A; such information can be very useful for the design of new inhibitors of κ-ORs.

1. Introduction

The main three families of plants with medicinal use in Argentina are *Asteraceae*, *Fabaceae*, and *Solanaceae*. Members of these families have been used for the prevention and relief of medical disorders since ancient time, therefore their metabolites have been extremely studied and an enormous amount of chemical information is now available [1–3]. In Argentina, *Asteraceae* comprises ca. 1490 species (indigenous and introduced) [4], and 272 native taxa (ca. 18%) have been reported with medicinal uses [5]. In particular, the genus *Baccharis* is one of the most important considering its enormous relevance regarding its medicinal, commercial, and biological applications [6]. Thirty-six species of the ninety-six growing in Argentine [7] have medicinal properties, and the majority of them have been phytochemically studied. *Baccharis* is an exclusively American genre, with around 500 species; most of them live in tropical regions of the continent, although there are many species of temperate and temperate-cold zones, some of which grow in the so-called Pampa Argentina. Some species of the genus *Baccharis* are known for the effect produced by their chemical principles. Thus, some of them, generically called “carquejas”, have an intensive use in popular medicine. Numerous studies have shown that the “carquejas” have antioxidant, anti-inflammatory, analgesic, anti-

Abbreviations: AMSL, Above mean sea level; i.p., Administered via the intraperitoneal route; ANMAT, Administración Nacional de Medicamentos, Alimentos y Tecnología Médica; CNS, Central nervous system; CTLC, Centrifugal thin layer chromatography; DAC, ent-15,16-epoxy-19-hydroxy-1,3,13(16),14-clerodatetraen-18-oic acid; DACD, (1R,4S,4aS,4bR,5S,6R,8aS,10aR)-3-(2-((1S,2R,4aS,8aR)-5-carboxy-4a-(hydroxymethyl)-1,2-dimethyl-1,2,3,4,4a,8a-hexahydronaphthalen-1-yl) ethyl)-5-(2-(furan-3-yl)ethyl)-8a-(hydroxymethyl)-5,6-dimethyl-1,4,4a,4b,5,6,7,8,8a,10a-decahydro-1,4-epoxyphenanthrene-9-carboxylic acid; MD, Molecular Dynamics; NO, Nitric oxide; SalA, Salvinorin A; *s.c.*, Subcutaneous; SAR, Structure-Activity Relationship; κ-ORs, κ-opioid receptors

* Corresponding author at: Instituto Multidisciplinario de Investigaciones Biológicas (IMIBIO-CONICET), Universidad Nacional de San Luis, Chacabuco 915, 5700 San Luis, Argentina.
E-mail address: denriz@unsl.edu.ar (R.D. Enriz).

https://doi.org/10.1016/j.fitote.2018.08.017
Received 2 July 2018; Received in revised form 13 August 2018; Accepted 22 August 2018
Available online 24 August 2018
0367-326X/

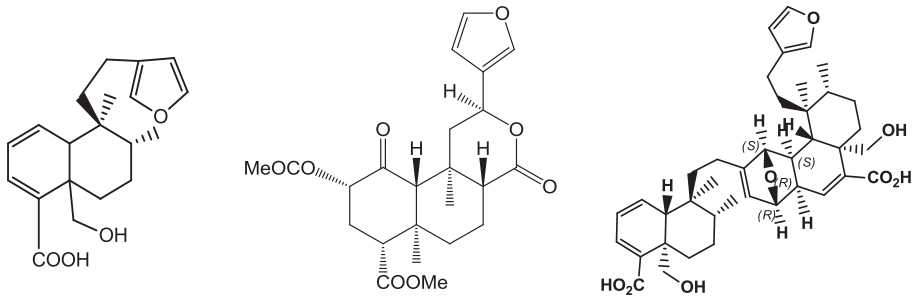

Fig. 1. Structures of **SalA, DAC** and its natural [4 + 2] photocycloaddition dimer **DACD**.

hepatotoxic and anti-mutagenic activities. Most of its uses in traditional medicine have been validated and these plants appear in the official pharmacopoeias of most of the countries of South America as specific plants for digestive aids. Gené et al. have reported that *B. trimera* shows strong anti-inflammatory and analgesic properties [8]. Very recently we have reported a dimer neoclerodane diterpene isolated from *B. flabellata* possibly formed by a [4 + 2] photo-cycloaddition of DAC (Fig. 1) called DACD [9]. Clerodane diterpenoids are a widespread class of secondary metabolites [10] which have been found in several plant species from various families as well as in organisms from other taxonomic groups such as fungi, bacteria, and marine sponges [11]. From a chemical point of view, clerodane diterpenes are bicyclic diterpenoids and their basic skeleton is divided into two fragments: a fused ring decalin moiety (C-1–C-10) and a six-carbon side chain at C-9. Clerodane diterpenoids constitute a large class of natural products and the number of these compounds has grown rapidly from several years ago. A comprehensive review on different aspects of clerodane diterpenoids was published by Li et al. [11]. Clerodane diterpenoids have attracted interest in recent years as a result of their noteworthy biological activities: antiparasitic [12], antifungal and antibacterial [13], antitumor [14] and anti-inflammatory [15]. In particular, much attention has been given to the antinociceptive activities found for SalA, non-nitrogenous opioid ligand of the κ-ORs [16,17].

Previous studies on the biological effects of essential oils obtained from *B. flabellata* have only reported antibacterial activities for *Staphylococcus aureus* [18]. However, neither analgesic nor antinociceptive activities have been reported to date for the extracts of any *Baccharis*. Having now the advantage of knowing about the presence of abundant amounts of DAC and DACD in the *B. flabellata* extracts, the question that arises is whether these extracts could have some type of antinociceptive activity. To answer this question, a study of the antinociceptive activity was made, taken the extracts at different times of the year, considering that the amount of DACD increases with the solar radiation. To complete this study, the activity of the supposed active principles DAC and DACD was also evaluated. In addition, we simulated the behavior of these clerodane diterpenoids over the k-ORs. From a molecular modeling study our results suggest that DAC and DACD act as agonists of the k-ORs. To better understand the effect at molecular level, combined techniques of docking and MD simulations have been used, which have allowed us to determinate the molecular interactions of these compounds at the molecular target. In this study we have also included SalA, which is a natural neoclerodane with potent opioid analgesic effect.

2. Material and methods

2.1. General experimental procedures

Solvents were analytical grade or were purified by standard procedures prior to use. Silica gel GF_{254} and Silica gel 60 (0.040–0.063 mm) were purchased at Merck (Darmstadt, Germany). ^{1}H and ^{13}C NMR spectra were performed on Bruker AC-200 spectrometer (200 MHz), 2D NMR spectra were measured as usual. We used $CDCl_3$ as solvent for ^{1}H and ^{13}C NMR spectra; chemical shifts were referenced to $CDCl_3$ residual signals, in the case of $CDCl_3$ at δ_H 7.26 and the central peak at δ_{13C} 77.0. EIMS: at 70 eV on GCQ Plus instrument. UV–Vis absorption spectra were taken with a Lambda 25 Perkin Elmer (Madrid, Spain) spectrometer.

2.2. Plant material and extraction procedure

Aerial parts (comprising leaves and stems, 100 g) of *B. flabellata* were collected during December of 2017 at 1270 m AMSL in Potrero de los Funes town, San Luis hills, Argentina (33° 11′ 90.88” S, 66° 15′ 42.63” W). All specimens were authenticated by Prof. Dr. Elisa Petenatti and each batch was deposited at the Herbarium of the Universidad Nacional de San Luis (L.A. Del Vitto & E.M. Petenatti # 9436). Leaves were extracted with methanol in portions of 200 ml each, immediately after being cut from the plant at room temperature.

2.3. Isolation of furan neoclerodanes

As it was previously reported [9], we employed here the same separative techniques. Thus, preparative TLC and Centrifugal TLC methods were employed to obtain DACD and DAC. Purity of isolated compounds was corroborated by HPLC-DAD, for details see Fig. S21 and S23 at Supplementary data.

2.4. Bioassays

2.4.1. Animals

The experiments were performed on Rockland mice of either sex (25–30 g) with free access to standard food and water, in a 12 h day–night cycle (lights on from 07:00 to 19:00 h), at a constant temperature of 22 ± 3 °C (with periodic cycles of air changes) and a relative humidity of about 50–60%. Acclimatization of animals was done for two days before the beginning of the experiment. The animals were randomly assigned to the different groups. All the animals were obtained from the Bioterium of the Facultad de Química, Bioquímica y Farmacia of Universidad Nacional de San Luis (Argentina) and the experiments were in compliance with the ANMAT No. 6344/96. [19] for animal care guidelines and were also authorized by Institutional Committee for the Care and Use of Laboratory Animals (Acronym: CICUA) of our institution (protocol No. F-206/15 in Resolution 324–16).

2.4.2. Antinociceptive activity

The hot-plate test was used to measure response latencies according to the method described by Eddy and Leimbach, with minor modifications [20]. Each mouse was placed on a hot plate kept at 56 ± 1 °C, after 30 min of animal's injections. The latency in seconds

was recorded using stop watch as the time between adjusting the animal on the hot plate and the appearance of symptoms of discomfort as licking the hind paws, shaking, or jumping off from the surface. The reaction time was recorded at 15, 30, 60 and 90 min after the treatments. The cutoff time of 60 s was selected according to Woolfe and MacDonald [21]. Mice with baseline latencies higher than 10 s were eliminated from the study. A significant increase of latency was considered as indicative of analgesic activity. One group of animals was treated with DAC and DACD at two doses (50 and 100 mg/kg, *i.p.*), another group was given morphine (10 mg/kg, *s.c.*); while control animals received the same volume of saline solution (10 ml/kg *i.p.*). To assess the possible participation of opioid receptors, mice were pretreated with naloxone (1 mg/kg *i.p.*), a non-selective antagonist of opioid receptors.

2.4.3. Statistical analysis

Statistical analysis was performed using GraphPad Prism version 5.00 for Windows and GraphPad InStat version 3.00 for Windows (GraphPad Software, San Diego, CA, USA, www.graphpad.com). Data were indicated as the mean ± standard error of the mean (SEM). The statistical significance of differences between groups was assessed by means of analysis of variance (ANOVA) and posterior comparison by Tukey. A probability of $p < .05$ was considered significant (section 4 of supplementary data).

2.5. Molecular modeling

2.5.1. Automated docking setup

AutoDock Vina 1.1.2 [22] was used to dock each compound to the κ-OR and all graphic manipulations and visualizations were performed using AutoDock Tools 1.5.6 [23]. The receptor structure corresponds to the following PDB code: 4DJH [24] (Wu et al., 2012). Missing residues Thr302, Ser303, His304, Ser305 and Thr306 have been included to the structure with Modeller 9.19 [25]. The receptor was defined as rigid, and the grid dimensions were 40, 40 and 40 for the X, Y and Z axes, respectively, in the active site region with a resolution of 0.375 Å. Nonpolar hydrogen atoms were merged and Gasteiger charges were assigned for all the compounds. All torsions of the ligands were allowed to rotate during docking. The value for the exhaustiveness of the search was 400, whereas the number of poses collected was 20.

2.5.2. MD simulations

MD simulations were performed using AMBER16 software package [26]. For each complex, the three lowest energy conformations from docking calculations were considered to carry out the MD simulations using periodic boundary conditions and cubic simulation cells with explicit water employing the TIP3P model [27]. The particle mesh Ewald method (PME) [28] was applied using a grid spacing of 1.2 Å, a spline interpolation order of 4 and a real space direct sum cutoff of 10 Å. The SHAKE algorithm [29] was applied allowing for an integration time step of 2 fs. MD simulations were carried out at 310 K and all alpha carbons from protein backbone were kept almost fixed with a harmonic force constant of 500 kcal/mol $Å^{-2}$. Three MD simulations of 5 ns were conducted for each system under different starting velocity distribution functions; thus, in total 15 ns were simulated for each complex. The NPT ensemble was employed using Berendsen coupling to a baro/thermostat (target pressure 1 atm, relaxation time 0.1 ps). Post MD analysis was carried out with program CPPTRAJ [30]. Spatial views shown in Figs. 2 and 4 were constructed using the UCSF Chimera program as a graphic interface [31].

2.5.3. MM-GBSA free energy decomposition

Histograms of interaction energy were used in order to determine which κ-OR residues are involved in the interactions with the ligands. For this purpose, we have employed MM-GBSA free energy decomposition using mm_pbsa program [32] in AMBER16. This calculation allows decomposing the interaction energies to each residue considering molecular mechanics and solvation energies [33]. Four energy terms are included for each ligand-residue pair: van der Waals contribution (ΔE_{vdW}), electrostatic contribution (ΔE_{ele}), polar desolvation term (ΔG_{GB}), and nonpolar desolvation term (ΔG_{SA}), which can be summarized as the following equation:

$$\Delta G_{ligand-residue} = \Delta E_{vdw} + \Delta E_{ele} + \Delta G_{GB} + \Delta G_{SA} \quad (1)$$

For MM-GBSA methodology, snapshots were taken at 10 ps time intervals from the corresponding last 2000 ps MD trajectories, and the explicit water molecules were removed from the snapshots.

3. Results and discussion

3.1. Antinociceptive activity of extracts of B. flabellata

In the first stage of our study, we evaluated the possible antinociceptive effects of *B. flabellata* extracts. It is interesting to note that the concentrations of DAC and DACD in the extracts vary during the different seasons of the year. In fact, during the summer months there is a markedly greater concentration of DACD with respect to DAC in the extracts; while during the winter months the exact opposite occurs (see Fig. S17, S18 and S19 in the supplementary data). This variation can be attributed mainly to solar radiation [9]. Therefore, for this study we have selected two extracts, one obtained in summer and another one during winter time. Our results indicate that both extracts show antinociceptive effects, with the extracts obtained during the summer being significantly more active (Table 1). These results are particularly interesting since in principle it is reasonable to think that the antinociceptive effect of DACD could be stronger than that of DAC (note the greater concentration of DACD in the extract of summer). To corroborate this hypothesis, the antinociceptive activities of DAC and DACD were evaluated. As expected, the DACD activities were significantly stronger than those obtained for DAC at the two concentrations evaluated here (see Table 1).

3.2. Antinociceptive activity of DAC and DACD

In a previous work, we showed that DAC and DACD are NO scavengers [9]. Based on these results, and in agreement with the scientifically evidence that some nitric oxide isoforms are considered atypical neurotransmitters of the CNS and they are related to pain generation [34], we assumed that DAC and DACD could produce antinociceptive effect. It should be noted that other neo-clerodane diterpenoids have also been reported as antinociceptive agents supporting our hypothesis [35].

The antinociceptive activities obtained for DAC and DACD are summarized in Table 1. As it can be observed, both compounds showed antinociceptive activity in the hot-plate test with DACD being significantly more active than DAC. So, in the hot-plate test, DAC (50 and 100 mg/kg, *i.p.*) and DACD (50 and 100 mg/kg, *i.p.*) increased the latency time of the animals compared to the control group ($p < .001$), after 30, 60 and 90 min of treatment, suggesting a possible antinociceptive activity mediated by central mechanisms. Morphine (50 and 100 mg/kg, *s.c.*) showed similar antinociceptive effect during the whole test (30–90 min).

On the other hand, the antinociceptive effect of DAC and DACD was reversed by prior administration of naloxone (1 mg/kg, *i.p.*), a non-selective antagonist of opioid receptors (Fig. 2), suggesting that the opioidergic mechanism is involved in the antinociceptive action of DAC and DACD.

At this point of our study we considered very important to determine the possible mechanism of action at molecular level of these compounds. Thus, considering the structural resemblance between DAC and DACD with SalA as well as the activities previously reported for neoclerodane diterpenoids on the κ-OR, it was reasonable to think that

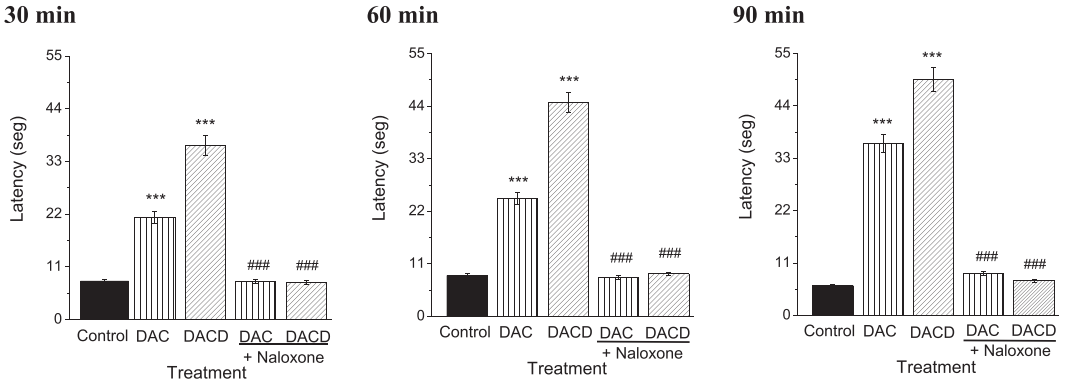

Fig. 2. Effect of **DAC** and **DACD** on hot plate test at 30, 60 and 90 min ($n = 7$) and pretreatment with naloxone (1 mg/kg, i.p.). All values were expressed as mean ± standard error of the mean (SEM). Asterisks denote significant differences from the control: $^{***}p < .001$ **DAC** and **DACD** alone vs. control (ANOVA and posterior comparison by Tukey); and $^{###}p < .001$ **DAC** and **DACD** + naloxone vs. control.

DAC and DACD could be acting against the same molecular target and through the same mechanism of action. Anyway it should be noted that we have not yet an experimental evidence indicating that DAC and DACD are binding to the κ-OR. Although our hypothesis might be considered somewhat speculative the above data support such idea. To corroborate this hypothesis, a molecular modeling study was performed in which DAC and DACD were simulated interacting at the active site of κ-OR. In this study, the SalA/κ-OR complex was also simulated to compare the results.

3.3. Molecular modeling

The combined analysis using a docking study and MD simulations predicts that DAC and DACD bind in the same region of the active site of κ-OR to that reported for SalA [36] (Fig. 3). These results can be well appreciated in the per residue analysis which has been performed on the different ligand-receptor complexes (Fig. 4); however, MD simulations indicate that these molecules are arranged spatially in a slightly different way.

While SalA (Fig. 4a) interacts mainly with Gln115, Trp139, Lys227, Ile294, Leu309, Tyr312 and Tyr313; DAC (Fig. 4b) produces their main interactions with Met142, Lys227, Trp287, Ile290, Ile294, Tyr312 and Tyr316. In turn, the main interactions stabilizing the complex of DACD (Fig. 4c) are those with Gln115, Val118, Tyr119, Asn122, Ser211, Lys227, Tyr312, Tyr313 and Ile316. Our results are in agreement with those previously reported for SalA [37] that indicate that the main stabilizing interactions of the complex are the following: Gln115, Leu135, Ile137, Leu212, His291, Ile294, Tyr312, Tyr313 and Ile316.

It is interesting to note that although the interaction with Lys227 is important for the three compounds under study and obviously it is present in the three histograms, this interaction is significantly stronger for DACD with respect to DAC and SalA (see Fig. 4). This interaction plus other strong interactions obtained for DACD such as with Gln115, Val118, Tyr119, Asn122 and Tyr313 might explain, at least in part, why DACD has more affinity for κ-OR than DAC. These results are in agreement with our experimental data. The above molecular interactions are stabilizing the different complexes and can be better appreciated in the Fig. 5.

The binding energies obtained from the MD simulations for the different complexes were − 37.56, − 21.07 and − 27.78 kcal/mol for SalA, DAC and DACD, respectively. Although we are comparing only three compounds, it should be noted that it is possible to find a correlation between the observed activities and the calculated binding energies. Note for example that DAC has a higher bond energy than DACD which agrees with the experimental results.

4. Conclusions

We report here for the first time antinociceptive activity for the extracts of *B. flabellata*; such activities are relatively strong, particularly those observed for the summer extract. Our results indicate that these activities are mainly due to the presence of DAC and DACD. These results suggest that analgesic activities previously reported for other *Baccharis* species could be due, at least in part, to the presence of this type of dimer, neoclerodanes and structurally related compounds.

Our results show that both DAC and DACD possess strong antinociceptive activity, especially DACD which displays a biological effect very similar to that of morphine. The demand for new agonists of the κ-

Table 1
The effect of Autumn Extract, Winter Extract, Summer Extract, **DAC**, **DACD** and morphine by i.p. or s.c. route of administration in the hot plate test. The latency for the nociceptive behavior was recorded at 15, 30, 60 and 90 min after the treatments. All values were expressed as mean ± standard error of the mean (SEM). Asterisks denote significant differences from the control: $^{***}p < .001$ vs. control (ANOVA and posterior comparison by Tukey).

Treatment	Dose (mg/kg)	15 min.	30 min.	60 min.	90 min.
Autumn Extract	50 *i.p.*	5.97 ± 0.48	16.05 ± 1.20***	18.05 ± 0.12***	20.05 ± 0.18***
	100 *i.p.*	7.52 ± 0.12	17.99 ± 0.72***	20.21 ± 0.69***	22.33 ± 0.63***
Winter Extract	50 *i.p.*	5.22 ± 0.24	8.54 ± 0.47***	10.35 ± 1.28***	15.58 ± 1.20***
	100 *i.p.*	8.17 ± 0.78	18.78 ± 1.52***	22.27 ± 0.83***	19.36 ± 1.00***
Summer Extract	50 *i.p.*	5.98 ± 0.61	9.65 ± 1.03***	16.77 ± 0.74***	27.28 ± 0.49***
	100 *i.p.*	7.98 ± 0.26	18.66 ± 0.95***	26.77 ± 1.38***	37.28 ± 0.25***
DAC	50 *i.p.*	7.97 ± 0.08	16.05 ± 0.52***	18.5 ± 0.30***	20.05 ± 0.5***
	100 *i.p.*	7.77 ± 0.48	16.68 ± 1.01***	21.08 ± 0.38***	24.60 ± 0.52***
DACD	50 *i.p.*	7.22 ± 0.36	22.31 ± 1.5***	32.0 ± 1.5***	39.22 ± 0.8***
	100 *i.p.*	7.64 ± 0.41	22.86 ± 1.15***	36.31 ± 1.08***	44.81 ± 1.39***
Morphine	50 *s.c.*	7.17 ± 0.19	31.85 ± 0.05***	49.10 ± 0.33***	52.8 ± 0.17***
	100 *s.c.*	8.10 ± 0.49	35.00 ± 0.07***	41.85 ± 0.45***	52.12 ± 0.83***
Control	Saline phys. Sol. *i.p.*	7.96 ± 0.37	8.20 ± 0.36	8.78 ± 0.25	8.43 ± 0.32

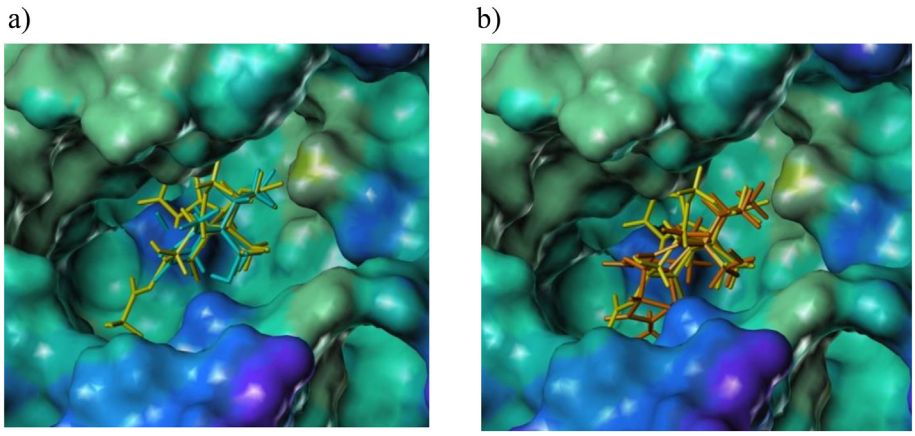

Fig. 3. Spatial view for a) the superimposition of the complexes **SalA** (yellow) and **DAC** (cyan); b) superimposition of the complexes obtained for **SalA** (yellow) and **DACD** (orange). An electrostatic potential surface of the binding site is shown in this figure, where red color denotes regions with negative charge density and blue color denotes regions with positive charge density. (For interpretation of the references to color in this figure legend, the reader is referred to the web version of this article.)

ORs and the new trend towards the use of natural products as medicines, instead of synthetic drugs, might open an alternative way for the development of new specific agonists of the κ-ORs. New analgesic agents could end up with the serious side-effects caused by morphine analgesic treatment, such as addictive tendency.

On the other hand, the results obtained from our study of molecular modeling have allowed us to understand the mechanism of action of DAC and DACD at molecular level. From our results it is also possible to explain the stronger activity obtained for the dimer DACD in comparison to DAC. Besides, our results have allowed us to appreciate some more subtle differences between possible molecular interactions of these ligands; such information can be certainly very useful for the design and search of new inhibitors of κ-ORs, whether from natural sources or obtained by synthesis.

Conflict of interest

The authors do not have any conflict of interest.

Acknowledgements

The continuous funding from the UNSL and CONICET is greatly appreciated by MF, RDE and RDT. The authors are grateful to PICTO-2017-19, Argentina for the financial support. Thanks are also due to Prof. Dr. Luis A. Del Vitto and Prof. Dr. Elisa Petenatti for the collaboration in the collection of plant specimens and for the botanical identification.

Conflict of interest

The authors have no conflict of interest.

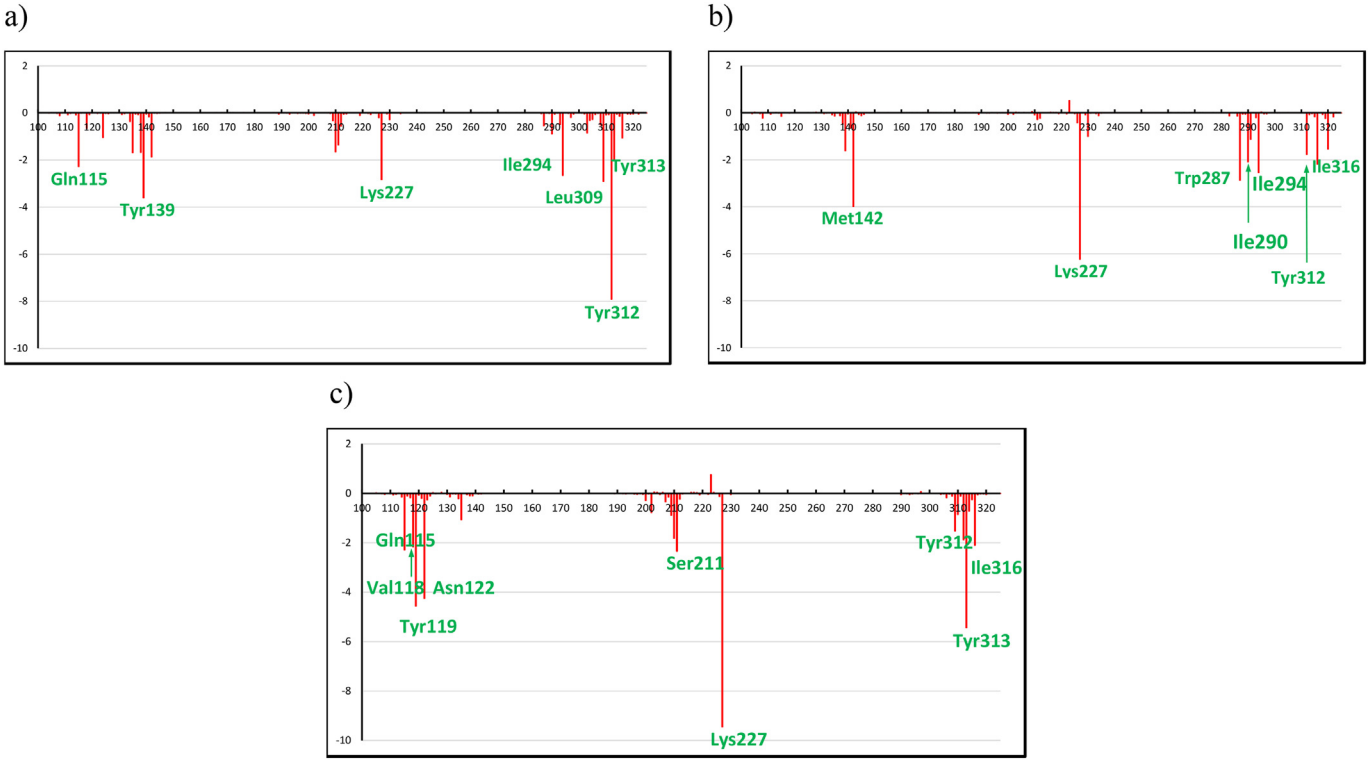

Fig. 4. Histograms of interaction energies partitioned with respect to the κ-OR amino acids in complex with **SalA** (a), **DAC** (b) and **DACD** (c). The *x-axis* denotes the residue number of κ-OR, and the *y-axis* denotes the interaction energy between the compounds and a specific residue. Negative values and positive values are favorable or unfavorable to binding, respectively.

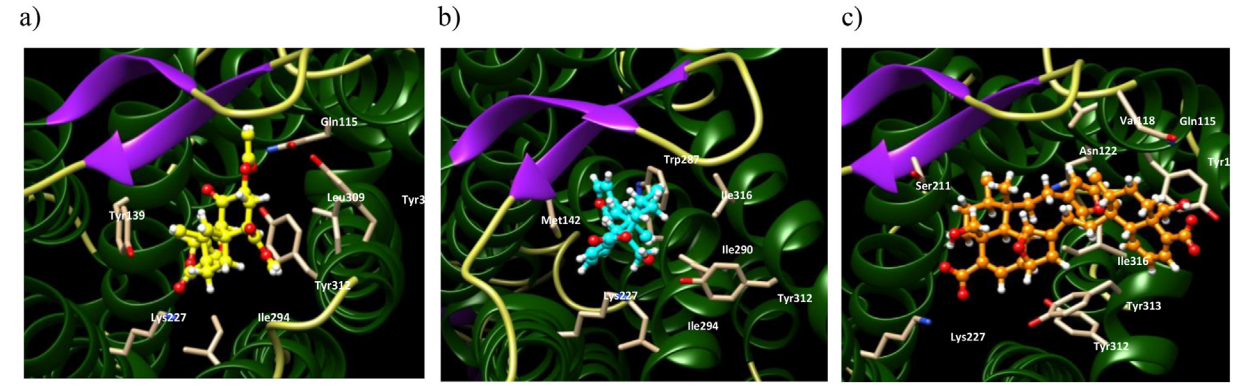

Fig. 5. Spatial view of the κ-OR binding site for the complexes with a) **SalA** (yellow); b) **DAC** (cyan) and c) **DACD** (orange). The different residues shown in these figures are involved in the main interactions stabilizing the three complexes. (For interpretation of the references to color in this figure legend, the reader is referred to the web version of this article.)

Appendix A. Supplementary data

Supplementary data to this article can be found online at https://doi.org/10.1016/j.fitote.2018.08.017.

References

[1] T.G. Payne, P.R. Jefferies, The chemistry of Dodonaea spp-IV diterpene and flavonoid components of D. attenuate, Tetrahedron 29 (1973) 2575–2583.

[2] V.P. Emerenciano, M.J.P. Ferreira, M.T. Scotti, M.V. Correia, S.A. Alvarenga, G.V. Rodrigues, Use of backpropagation artificial neural networks to predict the occurrences of chemical classes in Asteraceae, XXVII Annual Meeting on Micromolecular Evolution, Systematics and Ecology Reflections on the Current Status of Chemosystematics. RPS-2, São Paulo, Brasil, 2007.

[3] H. Wagner, Pharmaceutical and economic uses of the Compositae, en V. H. Heywood, J. B. Harborne & B. L. Turner (eds.), The Biology and Chemistry of the Compositae I, Academic Press INC, London, 1977, pp. 412–433.

[4] F.O. Zuloaga, O. Morrone, M.J. Belgrano, Catálogo de Plantas Vasculares del Cono Sur (Argentina, Sur de Brasil, Chile, Paraguay y Uruguay), Vol. 1–3 Missouri Botanical Garden, Saint Louis, Missouri, 2008.

[5] M.J. Abad, P. Bermejo, *Baccharis* (Compositae): a review update, ARKIVOC 7 (2007) 76–96.

[6] J.K. Bastos, Chemistry of *Baccharis* genus, Conferences Abstracts XX Simpósio de Plantas Medicinais do Brasil & X International Congress of Ethnopharmacology, 2008, p. 30 São Paulo, Brasil.

[7] D.A. Giuliano, Asteraceae, Tribu III. Astereae, parte A. Subtribu Baccharinae. Flora Fanerogámica Argentina 66, PROFLORA-CONICET, 2000, pp. 1–73.

[8] R.M. Gené, C. Cartaña, T. Adzet, E. Marín, T. Parella, S. Cañigueral, Anti-inflammatory and analgesic activity of *Baccharis trimera*: identification of its active constituents, Planta Med. 62 (1996) 232–235.

[9] M. Funes, C.E. Tonn, M. Kurina-Sanz, In vivo photoinduced [4 + 2] dimerization of a neo-clerodane diterpene in Baccharis flabellata. ROS and RNS scavenging abilities, J. Photochem. Photobiol. B 186 (2018) 137–143. Accepted for publication.

[10] T. Tokoroyama, Synthesis of clerodane diterpenoids and related compounds stereoselective construction of the decalin skeleton with multiple contiguous stereogenic centers, Synthesis 5 (2000) 611–633.

[11] R. Li, S.L. Morris-Natschkeb, L. Kuo-Hsiung, Clerodane diterpenes: sources, structures, and biological activities, Nat. Prod. Rep. 33 (2016) 1121–1122.

[12] D.D. Bou, A.G. Tempone, E.G. Pinto, J.H.G. Lago, P. Sartorelli, Antiparasitic activity and effect of casearins isolated from Casearia sylvestris on Leishmania and Trypanosoma cruzi plasma membrane, Phytomedicine 21 (2014) 676–681.

[13] V.K. Gupta, S. Verma, A. Pal, S.K. Srivastava, P.K. Srivastava, M.P. Darokar, In vivo efficacy and synergistic interaction of 16α-hydroxycleroda-3, 13 (14) Z-dien-15, 16-olide, a clerodane diterpene from Polyalthia longifolia against methicillin-resistant Staphylococcus aureus, Appl. Microbiol. Biotechnol. 97(2014)9121–9131.

[14] E.J. Ferreira De Araújo, A.A. Cardoso De Almeid, O. Almeida Silva, I.H. Fernandes Da Costa, L.M.J. Rezende, F. Das Chagas Alves Lima, L. Da Silva Lopes, A.J. Cavalheiro, P.M. Pinheiro Ferreira, Physiological behavioral changes induced by a fraction with antitumor cleronade diterpenes from an Atlantic forest Brazilian plant and computational intermolecular interactions with neuron receptors, J. Ethnopharmacol. 198 (2017) 460–467.

[15] E.G. Pierri, R.C. Castro, E.O. Vizioli, C.M.R. Ferreira, A.J. Cavalheiro, A.G. Tininis, C.M. Chin, A.G. Santos, Anti-inflammatory action of ethanolic extract and clerodane diterpenes from Casearia sylvestris, Rev. bras. farmacogn. 27 (2017) 495–501.

[16] T.E. Prisinzano, R.B. Rothman, Salvinorin A analogs as probes in opioid pharmacology, Chem. Rev. 108 (2008) 1732–1743.

[17] A. Cruz, S. Domingo, E. Gallardo, A. Martinho, A unique natural selective kappa-opioid receptor agonist, salvinorin A, and its roles in human therapeutics, Phytochemistry 137((2017) 9–14.

[18] M. Demo, M. de las M. Oliva1, M.L. Lopez, M.P. Zunino, A.J. Zygadlo, Antimicrobial Activity of Essential Oils Obtained from Aromatic Plants of Argentina, Pharm. Biol. 43 (2005) 129–134.

[19] Disposición No. 6344/96, Published in the Official Bulletin of the Nation No. 28567, 1st. Section January 20, 1997, Buenos Aires, Argentina. (ANMAT), (1996).

[20] N.B. Eddy, D. Leimbach, Synthetic analgesics. II. Dithienylbutenyl- and dithienylbutylamines, JPET. 107 (1953) 385–393.

[21] G. Woolfe, A.D. MacDonald, The evaluation of the analgesic action of pethidine hydrochloride, J. Pharmacol. Exp. Ther. 80 (1944) 300–307.

[22] O. Trott, A.J. Olson, AutoDock Vina: improving the speed and accuracy of docking with a new scoring function, efficient optimization, and multithreading, J. Comput. Chem. 31 (2010) 455–461.

[23] G.M. Morris, R. Huey, W. Lindstrom, M.F. Sanner, R.K. Belew, D.S. Goodsell, A.J. Olson, AutoDock4 and AutoDockTools4: automated docking with selective receptor flexibility, J. Comput. Chem. 30 (2009) 2785–2791.

[24] H. Wu, D. Wacker, M. Mileni, V. Katritch, G.W. Han, E. Vardy, W. Liu, A.A. Thompson, X.P. Huang, F.I. Carroll, S.W. Mascarella, R.B. Westkaemper, P.D. Mosier, B.L. Roth, V. Cherezov, R.C. Stevens, Structure of the human kappa-opioid receptor in complex with JDTic, Nature 485 (2012) 327–332.

[25] A. Sali, T.L. Blundell, Comparative protein modelling by satisfaction of spatial restraints, J. Mol. Biol. 234 (1993) 779–815.

[26] D.A. Case, D.S. Cerutti, T.E.I.I.I. Cheatham, T. Darden, R.E. Duke, T.J. Giese, H. Gohlke, A.W. Goetz, D. Greene, N. Homeyer, S. Izadi, A. Kovalenko, T.S. Lee, S. Legrand, P. Li, C. Lin, J. Liu, T. Luchko, R. Luo, D. Mermelstein, K.M. Merz, G. Monard, H. Nguyen, I. Omelyan, A. Onufriev, F. Pan, R. Qi, D.R. Roe, A. Roitberg, C. Sagui, C.L. Simmerling, W.M. Botello-Smith, J. Swails, R.C. Walker, J. Wang, R.M. Wolf, X. Wu, L. Xiao, D.M. York, P.A. Kollman, Amber16, University of California, San Francisco, 2017.

[27] W. Jorgensen, J. Chandrasekhar, J. Madura, R. Impey, M. Klein, Comparison of simple potential functions for simulating liquid water, J. Chem. Phys. 79 (1983) 926–935.

[28] T. Darden, D. York, L. Pedersen, Particle mesh Ewald - an N.log(n) method for Ewald sums in large systems, J. Chem. Phys. 98 (1993) 10089–10092.

[29] S. Miyamoto, P. Kollman, SETTLE-an analytical version of the shake and rattle algorithm for rigid water models, J. Comput. Chem. 13 (1992) 952–962.

[30] D.R. Roe, T.E. 3rd Cheatham, PTRAJ and CPPTRAJ: Software for processing and analysis of molecular dynamics trajectory data, J. of Chem. Theory and Compu. 9(2013)3084–3095.

[31] E.F. Pettersen, T.D. Goddard, C.C. Huang, G.S. Couch, D.M. Greenblatt, E.C. Meng, T.E. Ferrin, UCSF Chimera–a visualization system for exploratory research and analysis, J. Comput. Chem. 25 (2004) 1605–1612.

[32] B.R.I.I.I. Miller, T.D.Jr McGee, J.M. Swails, N. Homeyer, H. Gohlke, A.E. Roitberg, MMPBSA.py: An Efficient Program for End-State Free Energy Calculations, Theory and Compu. 8 (2012) 3314–3321.

[33] T. Hou, N. Li, Y. Li, W. Wang, Characterization of domain-peptide interaction interface: prediction of SH3 domain-mediated protein-protein interaction network in yeast by generic structure-based models, J. Proteome Res. 11 (2012) 2982–2995.

[34] M. Mittal, M.R. Siddiqui, K. Tran, S.P. Reddy, A.B. Malikcorresponding, Reactive oxygen species in inflammation and tissue injury, Antioxid. Redox Signal. 20 (2014) 1126–1167.

[35] A.E. Maqueda, The Use of Salvia divinorum from a Mazatec Perspective, in: B. Labate, C. Cavnar (Eds.), Plant Medicines, Healing and Psychedelic Science, Springer, Cham., New York, 2018, pp. 55–70.

[36] E. Vardy, P.D. Mosier, K.J. Frankowski, H. Wu, V. Katritch, R.B. Westkaemper, J. Aube, R.C. Stevens, B.L. Roth, Chemotype-selective modes of action of kappa-opioid receptor agonists, J. Biol. Chem. 288 (2013) 34470–34483.

[37] G. Leonis, A. Avramopoulos, R.E. Salmas, S. Durdagi, M. Yurtsever, M.G. Papadopoulos, Elucidation of conformational states, dynamics, and mechanism of binding in human kappa-opioid receptor complexes, J. Chem. Inf. Model. 54 (2014) 2294–2308.